Geotechnical Site Characterization, Robertson & Mayne (eds) © 1998 Balkema, Rotterdam, ISBN 90 5410 939 4

Delineation of densified sand at Treasure Island by SASW testing

R.D.Andrus & R.M.Chung
Building and Fire Research Laboratory, National Institute of Standards and Technology, Gaithersburg, Md., USA
K.H.Stokoe, II & J.A.Bay
Department of Civil Engineering, The University of Texas at Austin, Tex., USA

ABSTRACT: Areas of improved and unimproved soil near berthing Pier 1 at Treasure Island, California, were investigated by the Spectral-Analysis-of-Surface-Waves (SASW) test. The upper 12 m of sand fill beneath the approach to the pier had been densified by a vibrating probe technique in 1985. The area of improved soil performed well during the 1989 Loma Prieta earthquake, while sinkholes, sand boils and cracks formed in the adjacent unimproved areas. The SASW tests were conducted on a 240 m-long alignment that extended across the area of improved soil. Average shear wave velocities determined for the densified and undensified sand fill below the water table were 192 m/s and 167 m/s, respectively. Two simplified liquefaction assessment procedures based on shear wave velocity correctly predicted no liquefaction for the densified sand, and marginal liquefaction for the undensified sand.

1 INTRODUCTION

Liquefaction of loosely deposited granular soils is a major cause of damage in earthquakes. Delineation of weak soil layers and prediction of their liquefaction potential are key inputs in the engineering design of new or retrofitted structures. This information is also essential for reliable estimation of economic losses during future earthquakes. When projects extend for great distances, such as lifelines and large building complexes, cost-effective evaluations of extensive areas are required. Screening techniques based on geology, hydrology, and soil conditions show promise for identifying areas requiring more rigorous analyses. However, even these areas requiring further analyses can be quite large.

One promising technique for spatially evaluating the liquefaction susceptibility of granular soils is the Spectral-Analysis-of-Surface-Waves (SASW) test. This test is an in situ seismic test for determining small-strain shear wave velocity, V_S, profiles of soil deposits and pavements (Stokoe and Nazarian, 1985; Stokoe et al., 1988; Gucunski and Woods, 1991; Stokoe et al., 1994). The SASW test does not require boreholes, and has the advantage of providing broad areal coverage. Testing can be performed at sites where minimal disturbance is required and where soils are difficult to sample. The use of V_S as an index of liquefaction potential is justified since both V_S and liquefaction potential are influenced by many of the same factors (e.g. void ratio, effective confining pressure, stress history, and geologic age). Thus, the SASW test is well suited for profiling large areas with the objective of developing two- or three-dimensional images of the subsurface.

In March 1996, SASW tests were conducted across an area of densified sand at Treasure Island, California. The site, called the Improved Soil Area (ISA) herein, is located on the south-eastern corner of the island, as shown in Figure 1. The principal objective of these tests was to evaluate the ability of the SASW test to rapidly delineate stratigraphy and assess liquefaction resistance of the densified and undensified sands over a significant lateral extent. This paper presents the two-dimensional stiffness profile at ISA along with the liquefaction evaluation.

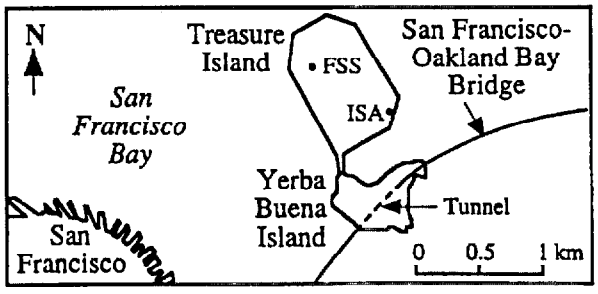

Figure 1. San Francisco Bay showing locations of the Improved Soil Area (ISA) and Fire Station Site (FSS) at Treasure Island.

Geotechnical Site Characterization Proceedings of the 1st International Conference on Site Characterization - ISC'98, April 19-22, 1998, Atlanta, GA. Edited by Peter K. Robertson and Paul W. Mayne. Published by A.A. Balkema/Rotterdam/Brookfield, Neterlands, Volume 1, 459-464, 1998.

1.1 *Treasure Island*

Treasure Island (TI) is a man-made island constructed in 1936-37. It was formed by hydraulic filling behind a perimeter rock dike. The perimeter dike served to contain the hydraulic fill, and was raised in sections over the previously placed fill. Currently, the island is occupied by the U.S. Navy.

In 1991, TI was selected as a national geotechnical experimentation site. Much of the work to date centers around a ground response experiment (de Alba and Faris, 1996). Six accelerometers and eight piezometers are operating at various elevations near the fire station (see Figure 1). Inclinometer casings are in place at the fire station and at two sites at the perimeter of TI, including the Improved Soil Area.

1.2 *Improved Soil Area*

The Improved Soil Area, shown in Figure 2, is essentially level and capped by a 127 mm-thick layer of asphalt. The upper 12 m of soil is sand fill initially deposited in a loose to medium dense state during hydraulic filling. Grain-size distribution curves for six samples taken from the fill are shown in Figure 3. Samples above a depth of 6 m contain as much as 17% fines (silt and clay). Below 6 m, samples contain 1% to 4% fines. The fill is underlain by 3 m of native silty clayey sand followed by 27 m of soft to stiff clay with interbedded sand layers. The clay is underlain by alternating layers of very stiff sandy clay and dense sand. Sandstone and shale bedrock occurs at a depth of 87 m at the fire station (de Alba and Faris, 1996). It is assumed that the bedrock surface slopes upward from the fire station to the sandstone rock forming Yerba Buena Island (see Figure 1). At the time of SASW testing, the water surface in the bay was about 2 m below the ground surface.

Because of concern for the seismic instability of the waterfront slope, the fill beneath the approach to Pier 1 was densified to a depth of 12 m by a vibrating probe technique in 1985. The area penetrated by the large metal-tube probe was 23 m wide and 97 m long, as shown in Figure 2. From construction drawings by Foundation Contractor Inc., initial tests were conducted at the northwest corner of the improved area to determine the optimal probe spacing. Subsequent production probes were performed to produce a final 1.90 m or 2.24 m probe spacing in a triangular grid pattern. Gravelly material was inserted through holes in the wall of the probe and vibrated into the ground. Curves 4-6 shown in Figure 3 are for samples taken from the improved zone.

Following the 1989 Loma Prieta earthquake (M_W = 7.0), no signs of ground disturbance were observed in the improved area, while sinkholes, sand boils and cracks were seen in the adjacent unimproved areas (Geomatrix, 1990; Mitchell and Wentz, 1991).

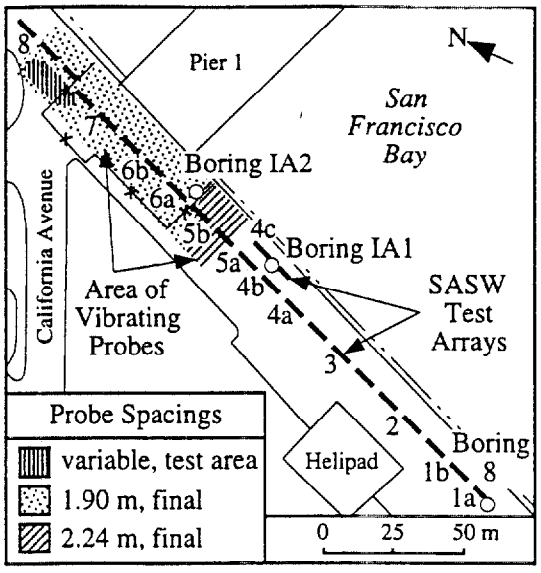

Figure 2. Improved Soil Area showing locations of structures (de Alba and Faris, 1996) and tests.

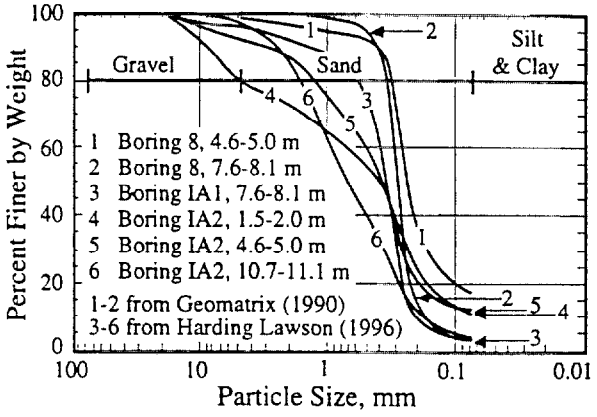

Figure 3. Grain-size distribution curves of six split-barrel samples taken from the sand fill.

2 SASW TEST

The SASW test is based on the principle that the extent of the soil profile sampled by surface waves varies with frequency (hence wavelength). Thus, if stiffness varies with depth, surface waves of different frequencies will propagate at different velocities.

Field tests were performed by placing two receivers on the ground surface a distance D apart, as illustrated in Figure 4. A truck-mounted seismic vibrator (or vibroseis) weighing 180 kN was used as the source for spacings over 8 m. For shorter spacings, hand-held hammers and dropped weights were used. The two receiver signals were recorded, and transformed into the frequency domain using a FFT signal analyzer. From the two frequency domain records, the coherence and the phase of the cross-power spectrum were computed.

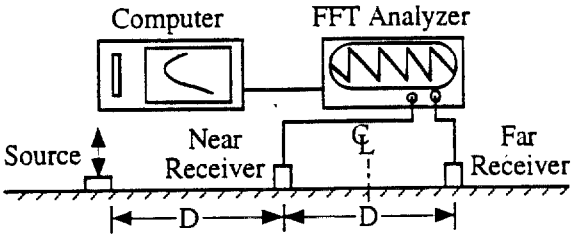

Figure 4. SASW test configuration.

Where data quality was good in the phase plot of the cross-power spectrum, Rayleigh wave phase velocity, V_R, and corresponding wavelength, λ_R, were calculated for each frequency by:

$$V_R = D(2\pi f)/\Phi \quad (1)$$

$$\lambda_R = V_R/f \quad (2)$$

where Φ is phase difference in radians, f is frequency in cycles per second, and π is a constant of about 3.14. A plot of V_R versus λ_R was assembled with the results for all receiver spacings. This plot is called the experimental dispersion curve.

Shear wave velocity profiles were obtained through an iterative process of matching the experimental dispersion curve to the theoretical dispersion curve. To begin this iterative process, initial properties (shear and compression wave velocities and total unit weights) and layer thicknesses were assumed. A theoretical dispersion curve was calculated for the assumed horizontally layered profile using the three-dimensional computer model by Roësset et al. (1991). The assumed properties (primarily V_S) and layer thicknesses were adjusted until satisfactory agreement between the theoretical and experimental dispersion curves was obtained. Agreement between the two dispersion curves was assessed visually and by a maximum likelihood method formulation (Joh 1996). The V_S-values and layer thicknesses for the final theoretical dispersion curve were then used to represent the actual profile of the site.

3 RESULTS

Experimental dispersion curves obtained for receivers spacings of 7.6 m, 15.2 m, and 30.5 m are plotted in Figure 5. The dispersion curves for test arrays in the improved area (solid symbols) are distinctly separated from the dispersion curves for test arrays in the unimproved area (open symbols). The dispersion curves for two arrays located 40-50% within the improved area (+ symbols) lie between the open and solid symbols, as shown in Figures 5b and 5c. Values of V_R for the improved area are as much as 90 m/s higher than values of V_R for the unimproved area at a wavelength of 3 m. This difference in V_R-values decreases to about 15 m/s at a wavelength of 30 m. Between wavelengths of 5 m and 24 m, the average difference in values of V_R is 31 m/s.

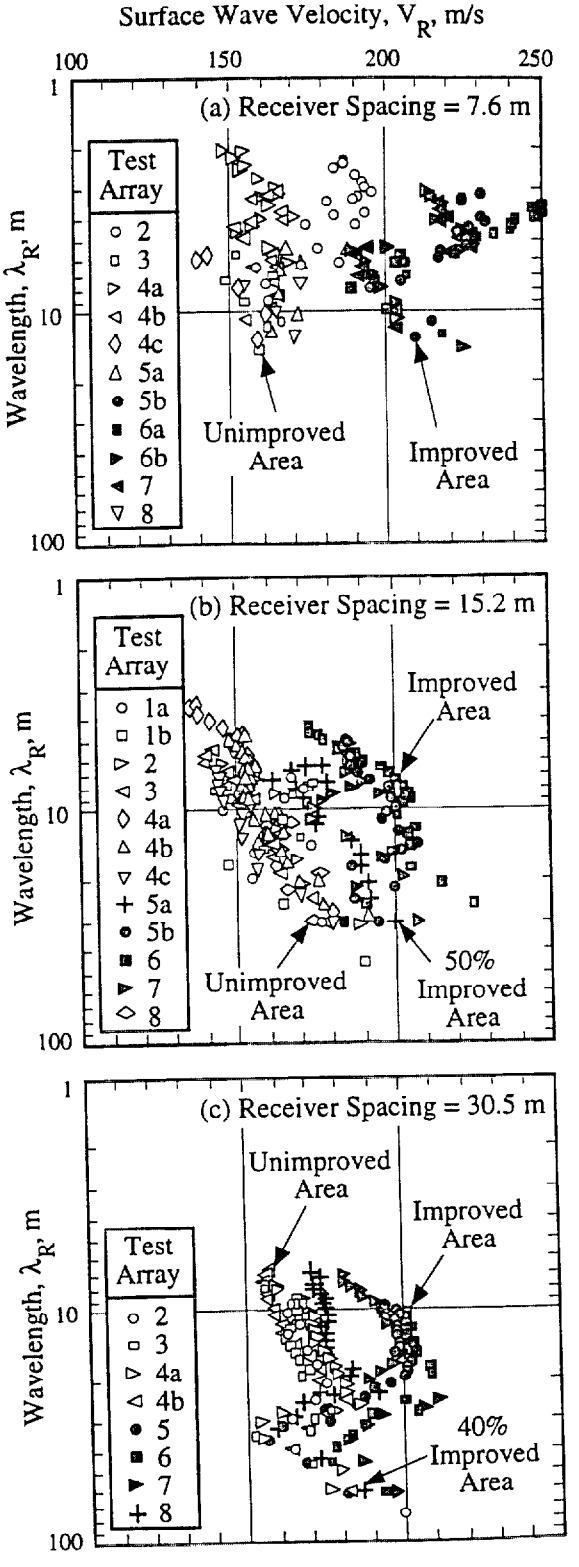

Figure 5. SASW experimental dispersion curves.

SASW test array 4c is located next to a sinkhole formed by liquefaction during the 1989 Loma Prieta earthquake. Values of V_R for test array 4c are among the lowest measured, as shown in Figures 5a and 5b. This observation was also expected, since array 4c lies closer to the waterfront slope (see Figure 2) where overburden pressures in underlying soil are lower.

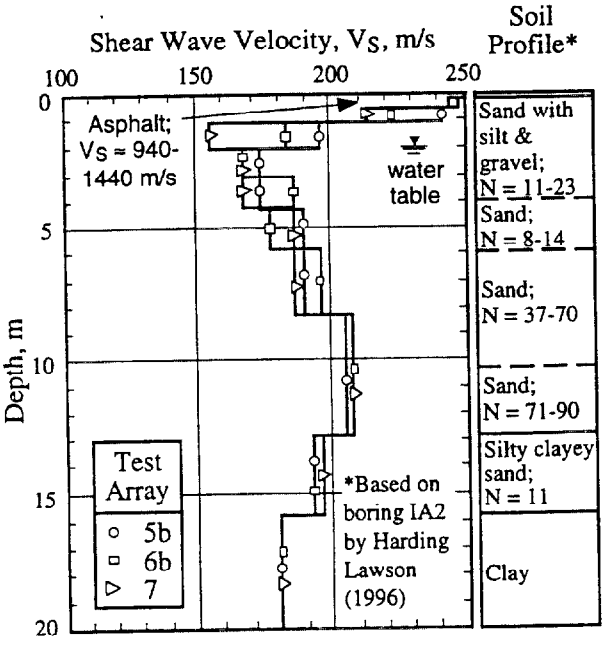

Figure 6. Three shear wave velocity profiles for SASW tests conducted in the improved area.

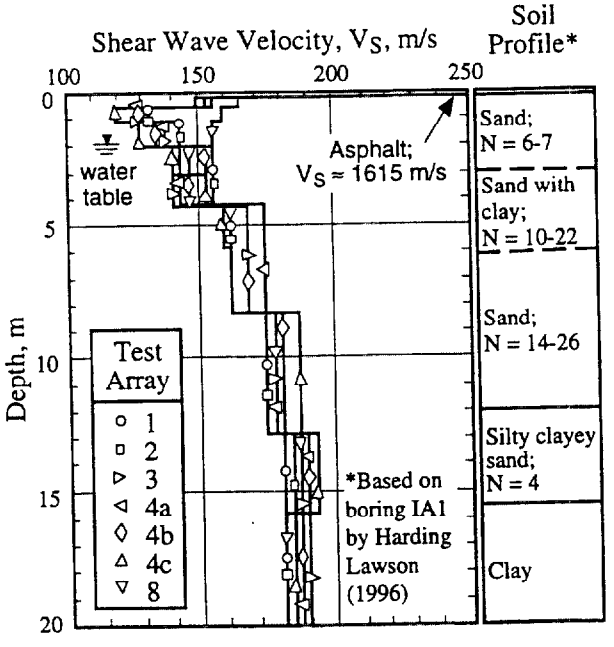

Figure 7. Seven shear wave velocity profiles for SASW tests conducted in the unimproved area.

Shear wave velocity profiles for SASW tests conducted in the improved and unimproved areas are shown in Figures 6 and 7, respectively. Values of V_S for the improved area are about 94 m/s higher than values of V_S for the unimproved area at a depth of 1 m (226 m/s versus 132 m/s). At a depth of 13 m, the difference between V_S-values is about 7 m/s (193 m/s versus 186 m/s). This trend is similar to the measurements of V_R (see Figure 5) and the Standard Penetration Test N-values given in Figures 6 and 7. A depth of 13 m agrees well the reported depth of densification of 12 m. Between the depths of 2 m and 13 m, average V_S-values for the undensified and densified fill are 167 m/s and 192 m/s, respectively.

Assembling the V_R- and V_S-profiles presented in Figures 5, 6 and 7 leads to the two-dimensional velocity profiles shown in Figure 8. Several test setups near the southern end of the improved area permit good resolution of the boundary separating densified and undensified sands. At the northern end of the improved area, however, the number of test setups are limited and the agreement between the velocity profiles and the lateral limit of vibrating probes is rather poor. Nevertheless, the zone of densified sand is clearly identified in both profiles.

Since the process for obtaining V_R-profiles is not computationally intensive, two-dimensional profiles, such as the one shown in Figure 8a, could be completed during field testing. For the measurements presented in this paper, field testing was completed

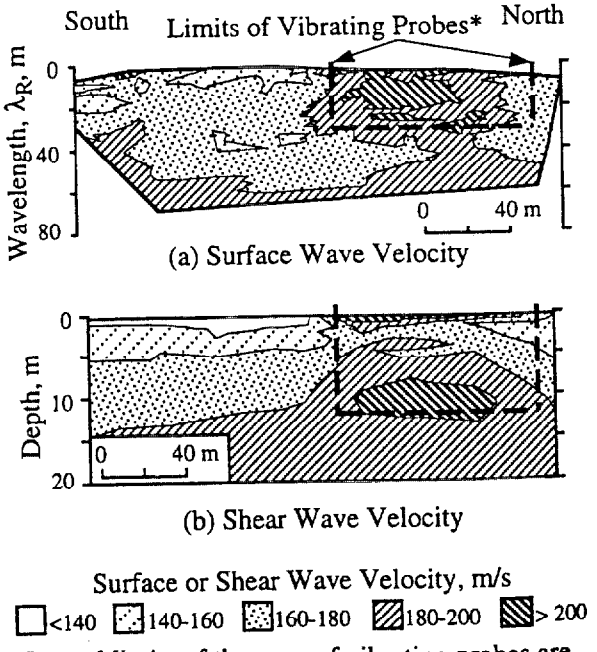

Figure 8. Two-dimensional velocity profiles.

within a 7-hour period. This time could be reduced once a routine is established. Thus, similar two-dimensional profiles with lengths of 500 m to 1000 m could be generated in a day.

The process for obtaining a single V_S-profile is computationally intensive, often requiring more than 8 hours of computer time to complete.

4 LIQUEFACTION ANALYSES

Several liquefaction assessment procedures based on V_S have been proposed during the past decade. These procedures are evaluated by Andrus and Stokoe (in press) using liquefaction and non-liquefaction case histories from 17 earthquakes and over 43 sites. From the case histories, modifications to earlier procedures are recommended. Shear wave velocity measurements from the ISA provide one of the first opportunities to apply these new procedures.

The recommended procedure follows the format of the penetration-based procedures, where penetration or V_S is correlated with the cyclic stress ratio (CSR). The CSR at a particular depth in a level soil deposit can be expressed as (Seed and Idriss, 1971):

$$\tau_{av}/\sigma'_v = 0.65(a_{max}/g)(\sigma_v/\sigma'_v)r_d \quad (3)$$

in which τ_{av} is cyclic shear stress generated by the earthquake, a_{max} is peak horizontal ground surface acceleration, σ'_v is initial effective vertical stress, σ_v is total vertical stress, g is acceleration of gravity, and r_d is a shear stress reduction factor with a value less than 1. Based on a_{max} of 0.16 g and 0.11 g recorded in the x and y directions at the fire station during the 1989 earthquake (Brady and Shakal, 1994), an average value of 0.14 g is used in the analyses. Vertical stresses are estimated using total unit weights of 17.3-18.9 kN/m^3 and 19.5-21.2 kN/m^3 for soils above and below the water table, respectively.

The shear wave velocity is corrected with respect to a reference stress, P_a, by (Robertson et al., 1992):

$$V_{S1} = V_S(P_a/\sigma'_v)^{0.25} \quad (4)$$

where P_a is typically 100 kPa and σ'_v in kPa.

Liquefaction in the unimproved soil most likely occurred where V_{S1} and fines content are least, and where CSR is greatest. These conditions occur between the depths of 6 m and 12 m.

Resistance to liquefaction caused by magnitude 7.5 earthquakes can be defined by (Andrus and Stokoe, in press; modified from Dobry, 1996):

$$\tau_l/\sigma'_v = a(V_{S1}/100)^2 + b[1/(V_{S1c}-V_{S1})-1/V_{S1c}] \quad (5)$$

where τ_l is cyclic shear stress resisting liquefaction, V_{S1c} is critical value of V_{S1} which separates contractive and dialative behavior, and "a" and "b" are factors with values approximately equal to 0.03 and 0.9, respectively. The value of V_{S1c} is about 220 m/s for uncemented soils with fines content less 5%. For magnitude 7 earthquakes, Equation 5 is multiplied by a scaling factor of about 1.2.

Using Equation 5, the boundary separating liquefaction and no liquefaction for magnitude 7 earthquakes is drawn in Figure 9. Also plotted in Figure 9 are average values of V_{S1} and CSR for the critical layer. The data for the improved area correctly lie in the region of no liquefaction. For the unimproved area, the data lie on the boundary, and marginal liquefaction is predicted. Located close to the perimeter of the island, sloping ground may have contributed to the amount of liquefaction effects. In addition, lateral ground displacement was only about 80 mm. Thus, a prediction of marginal liquefaction for the unimproved area is considered correct.

Another method relating liquefaction potential and V_S has evolved from the strain approach by Dobry et al. (1982) and the analytical studies by Stokoe et al. (1989). By combining Equations 3, 4 and 5, a relationship based on V_S and a_{max} is obtained in the form of (Andrus and Stokoe, in press):

$$a_{max}/g = f_1\{a(f_2V_S/100)^2 + b[1/(V_{S1c}-f_2V_S)-1/V_{S1c}]\} \quad (6)$$

where $f_1 \approx 1.1/r_d$ and $f_2 \approx (7.3/z)^{0.25}$, and z is depth to center of the critical layer in meters. This formulation assumes the water table is located midway between the ground surface and the center of the critical layer, and the total unit weights of soil above and below the water table are 17.3 kN/m^3 and 18.9 kN/m^3, respectively. The boundary for magnitude 7 earthquakes and depth of 9 m is shown in Figure 10. Liquefaction behavior predicted by this method is similar to the method based on V_{S1} and CSR.

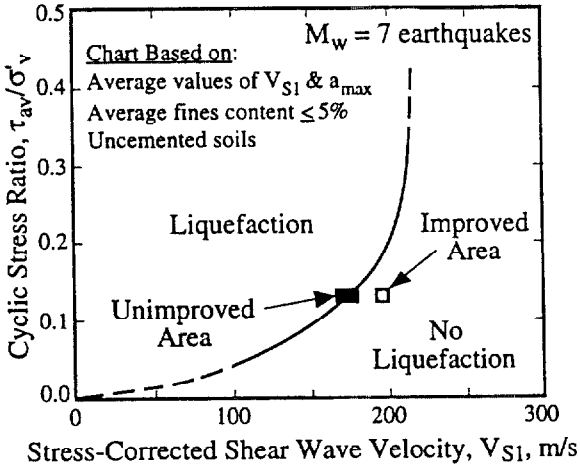

Figure 9. Comparison of liquefaction assessment chart based on V_{S1} and CSR (Andrus and Stokoe, in press) with results from ISA.

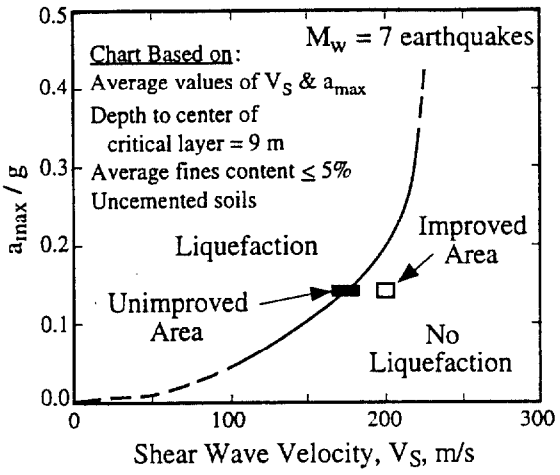

Figure 10. Comparison of liquefaction assessment chart based on V_S and average a_{max} (Andrus and Stokoe, in press) with results from ISA.

CONCLUSIONS

The zone of densified sand adjacent to Pier 1 at TI was correctly identified in V_R- and V_S-profiles obtained from SASW tests. Velocities measured in the improved area were about 30 m/s greater than velocities measured in the unimproved area. Two liquefaction assessment procedures based on V_S correctly predicted no liquefaction for the improved area, and marginal liquefaction for the unimproved area. This study further supports the usefulness of in situ V_S for predicting liquefaction potential, and demonstrates the potential of the SASW test for rapid delineation of weak layers. For large study areas, a cost-effective investigation program might be to first develop profiles of V_R in the field (assuming an approximate sampling depth equal to $\lambda_R/3$ to $\lambda_R/2$). The V_R-profiles would then be used to select locations for determining V_S-profiles and sites for borehole sampling and penetration testing.

ACKNOWLEDGEMENTS

The authors gratefully acknowledge the assistance of Richard Faris, Naval Facilities Engrg. Command, for scheduling tests and supplying site data. The help of Brent Rosenblad with field work and Sung-Ho Joh with data reduction is also greatly appreciated. We also thank Glenn Rix, Georgia Tech., for his review.

REFERENCES

Andrus, R.D. & K.H. Stokoe, II in press. Liquefaction resistance based on shear wave velocity, *Workshop on Evaluation of Liquefaction Resistance*, Jan. 1996, NCEER, Buffalo, N.Y.

Brady, A.G. & S.F. Shakal 1994. Strong-motion recordings, *USGS Prof. Paper 1551-A*, R. Borcherdt, ed., U.S. Gov. Printing Office, Washington, D.C., 9-38.

de Alba, P. & J.R. Faris 1996. Current state of site characterization and instrumentation, Treasure Island, Calif., *Workshop on Future Res. Deep Instrumentation Array TI, NGES*, Univ. of N.H.

Dobry, R. 1996. Personal communication.

Dobry, R., R.S. Ladd, F.Y. Yokel, R.M. Chung & D. Powel 1982. Prediction of pore water pressure buildup and liquefaction of sands during earthquakes by the cyclic strain method, *NBS Bldg. Sci. Series 138, U.S. Dept. of Commerce.*

Geomatrix Consultants 1990. Evaluation of interior area performance, Naval Station Treasure Island, San Francisco, Calif., Vol. 1-5.

Gucunski, N. & R.D. Woods 1990. Instrumentation for SASW testing, *Geotech. Special Pub. No. 29*, S.K. Bhatia & G.W. Blaney, eds., ASCE, New York, N.Y., 1-16.

Harding Lawson Associates 1996. National geotechnical experimentation site, soil boring and sampling, phase II, San Francisco, Calif.

Joh, S.-H. 1996. Advances in interpretation and analysis techniques for Spectral-Analysis-of-Surface-Wave (SASW) measurements, *Ph.D. Dissertation*, Univ. Tex. at Austin.

Mitchell, J.K. & F.J. Wentz, Jr. 1991. Performance of improved ground during the Loma Prieta earthquake, *Rep. No. UCB/EERC-91/12*, Univ. of Calif., Berkeley.

Robertson, P.K., D.J. Woeller & W.D.L. Finn 1992. Seismic cone penetration test for evaluating liquefaction potential under cyclic loading, *Can. Geotech. J.*, Ottawa, Canada, 29, 686-695.

Roësset, J.M., D.W. Chang & K.H. Stokoe, II, 1991. Comparison of 2-D and 3-D models of analysis of surface wave tests, *Proc. 5th ICSDEE*, Karlsruhe, Germany, 111-126.

Seed, H.B. & I.M. Idriss 1971. Simplified procedure for evaluating soil liquefaction potential, *J. Soil Mechanics and Found. Div.*, ASCE, New York, N.Y., 105:2, 1249-1273.

Stokoe, K.H., II & S. Nazarian 1985. Use of Rayleigh waves in liquefaction studies, *Measurement and Use of Shear Wave Velocity for Evaluating Dyn. Soil Properties*, ASCE, New York, N.Y., 1-17.

Stokoe, K.H., II, S. Nazarian, G.J. Rix, I. Sanchez-Salinero, J.-C. Sheu & Y.-J. Mok 1988. In situ seismic testing of hard-to-sample soils by surface wave method, *Geotech. Special Pub. No. 20*, J.L. Von Thun, ed., ASCE, New York, N.Y., 264-278.

Stokoe, K.H., II, J.M. Roësset, J.G. Bierschwale & M. Aouad 1989. Liquefaction potential of sands from shear wave velocity, *Proc. 9th WCEE III*, Tokyo, Japan, Nissei Kogyo Co., Ltd, 213-218.

Stokoe, K.H., II, S.G. Wright, J.A. Bay & J.M. Roësset 1994. Characterization of geotechnical sites by SASW method, *Geophysical Characterization of Sites*, R.D. Woods, ed., IBH Oxford Press, New Delhi.